RSC Advances

ROYAL SOCIETY OF CHEMISTRY

www.rsc.org/advances

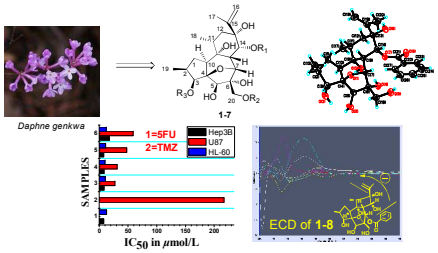

Neogenkwanines A–H: Daphnane-Type Diterpenes Containing 4,7 or 4,6-Ether Group from the Flower Bud of *Daphne genkwa*

Ling-Zhi Li[a,b], Shao-Jiang Song [a,b,*] , Pin-Yi Gao[c], Fei-Fei Li[a,b], Li-Hui Wang[d], Qing-Bo Liu[a,b], Xiao-Xiao Huang[a,b], Dan-Qi Li[a,b], Yu Sun[a,b]

[a] *School of Traditional Chinese Materia Medica, Shenyang Pharmaceutical University. 103 Wenhua Rd., Shenyang 110016, People's Republic of China*

[b] *Key Laboratory of Structure-Based Drug Design and Discovery, Ministry of Education, Shenyang Pharmaceutical University, 103 Wenhua Rd., Shenyang 110016, People's Republic of China*

[c] *College of Pharmaceutical and Biological Engineering, Shenyang University of Chemical Technology, Shenyang 110142, People's Republic of China*

[d] *School of Life Science and Biopharmaceuticals, Shenyang Pharmaceutical University. 103 Wenhua Rd., Shenyang 110016, People's Republic of China*

[*]*To whom correspondence should be addressed. (S.-J. Song) E-mail: songsj99@163.com. Tel: +86–24–23986088 Fax: +86–24–23986510*

† Electronic supplementary information (ESI) available: The ^{1}H NMR, ^{13}C NMR, HSQC, HMBC and NOESY spectra of compounds **1–9**, the HRESIMS, CD spectra of **1–8**, as well as CIF data for compound **1**. For ESI and crystallographic data in CIF or other electronic format see DOI:

ABSTRACT

Neogenkwanines A–H (**1–8**), eight daphnane-type diterpenes possessing new skeletons with 4,7- or 4,6-ether group, along with seven known ones (**10–16**), were isolated from *Daphne genkwa*. Their structures and absolute configurations were established by analysis of their NMR, X-ray crystallography, CD exciton chirality data and hydrolysis experiments. In addition, an MTT assay was used to examine the growth-inhibitory effects of all the new isolates on HL-60, Hep3B, and U87 cells; Compounds **3**, **4** and **5** exhibited significant inhibitory effects against Hep3B cell lines with IC_{50} values of 7.61, 8.16 and 8.35 μM, respectively.

Keywords: daphnane-type diterpene, hydrolysis, *Daphne genkwa,* bioactivity

Introduction

Plants from the Thymelaeaceae and Euphorbiaceae families contain structurally unique diterpenes belonging to the daphnane skeletal types.[1,2] Daphnanes include one or more of the oxygen atoms in a cyclic system and therefore can be regarded as heterocyclic compounds. Most of the daphnanes possessing a ring C-orthoester function exhibit various physiological activities, such as antileukemic, neurotrophic, tumor promoting, skin irritant, antifertility and insecticidal activities.[3-5] So far, more than 150 daphnane-type diterpenes have been isolated.[2,6,7] Among them, many diterpenes derived from the flower buds of *Daphne genkwa* Sieb. et Zucc. (Thymelaeaceae), a well-known Chinese folk medicine which has been evaluated clinically as an abortifacient.[8,9] Several reviews have been published covering the development of diterpenes from *D. genkwa* in the last two decades, highlighting their marked antitumor activity,[2, 10-12] and more recently, our current study identified a novel mechanism underlying anti-cancer effect of yuanhuacine (YHL–14, the major daphnane diterpene ester of *D. genkwa*.), showing that it inhibited bladder and colon cancer cell growth through up-regulation of p21 expression.[13] In our latest research, eight novel daphnane-type diterpenes neogenkwanines A–H (**1–8**) with a highly oxygenated skeleton featuring a rare 4,7- or 4,6-ether group were isolated from the flower buds of *D. genkwa*. This report describes the isolation, structural elucidation, plausible biogenetic pathways, and biological activities of these compounds.

Results and discussion

The ethanolic extract of *Daphne genkwa* flower buds was fractionated using different organic solvents to yield three fractions. Bioassay-guided fractionation utilizing TLC analysis of the cytotoxic assay indicated that CH_2Cl_2-soluble fraction is the most active layer. Silica gel normal and reversed-phase column chromatography and followed by HPLC purication of selected

fractions led to the isolation of eight new metabolites, neogenkwanines A–H (**1–8**) as well as seven known ones, including: genkwanine A (**10**),[11] genkwanine D (**11**),[11] genkwanine H (**12**),[11] yuanhuacine (**13**),[14] daphnane-type diterpene ester-7 (**14**),[15] genkwanine M (**15**),[11] genkwanine J (**16**).[11]

Neogenkwanine A (**1**), $[\alpha]_D^{22}$ −14.9 (*c* 2.2, $CHCl_3$), obtained as colorless crystals, had a molecular formula of $C_{27}H_{36}O_9$ as determined by the HRESIMS ion at *m/z* 527.2253 $[M+Na]^+$ (calcd 527.2252) with 10 degrees of unsaturation. In the ^1H NMR spectrum (Table 1), typical signals of the diterpene unit were identified. The presence of one tertiary methyl at δ_H 1.92 (3H, s), and two secondary methyls at δ_H 0.96 (3H, d, J = 6.6 Hz) and 0.98 (3H, d, J = 7.2 Hz) were revealed, and there was one oxygenated methylene at δ_H 3.47 (1H, d, J = 11.4 Hz) and 3.95 (1H, d, J = 11.4 Hz). The olefinic H-atoms appeared to be at a terminal double bond [δ_H 5.20 (1H, s) and 5.19 (1H, s)], while five aromatic H-atoms at δ_H 8.03–7.44 indicated the presence of one phenyl moiety. The ^{13}C NMR spectrum (Table 1) exhibited 27 carbon resonances, from which, three methyls, one terminal double bond, and one phenyl group were identified. Compared with daphnetoxin (**c**) [16], the first daphnane skeleton to be identified, compound **1**, had different oxygenation pattern of ring C, the absence of the typical orthoester group, and the presence of one ester carbonyl at δ_C 166.6 in **1** suggesting that a benzoyloxy group was likely located at C-14 and two hydroxyls were linked to the C-9 and C-13. The significant downfield shifted H-14 proton signal at δ 5.79 proved the presence of a benzoyl group at C-14, and the position of the benzoate substituent was further confirmed by HMBC experiment (Figure 1), in which, a long-range correlation between H-14 and the carbonyl group at δ_C 166.6 was observed. The above functionalities accounted for 6 degrees of unsaturation, and the remaining 4 degrees of unsaturation required that compound **1** was tetracyclic in the diterpene core. In the HMBC

spectrum (Figure 1), the proton signals at δ_H 0.96 (CH_3-19) correlated with the carbon signal at δ_C 34.9 (C-1), 31.9 (C-2), 74.3 (C-3), CH_3-18 at δ_H 0.96 showed correlations with δ_C 49.0 (C-10) and 35.8 (C-11), H-2 at δ_H 1.97 correlated with δ_C 74.3 (C-3), 71.8 (C-9), and H-7 at δ_H 3.90 correlated with δ_C 90.4 (C-4) and 71.8 (C-9), were allowed the identification of the typical A, B and C rings which accounted for 3 degrees of unsaturation. The last unsaturation was displayed by an additional oxetane ring which was most likely formed between two carbons at δ_C 90.4 (C-4) and 80.5 (C-7), since they were markedly downfield shifted, and a long range correlation between the carbon signal at δ_C 90.4 (C-4) and the proton signal at δ_H 3.90 (H-7) was observed in the HMBC spectrum (Figure 1). This completed the assignment of the planar structure of neogenkwanine A (**1**), as depicted.

The relative configuration of **1** was confirmed by the ^{1}H NMR coupling constants and the correlations in its NOESY plot (Figure 1). The vicinal coupling constant $J_{(2,3)}$ of 10.2 Hz suggested a *cis* relationship between the protons H-2 and H-3. Regarding the crucial NOE correlation between H-2/H-10, and H-10/H-5 this suggested that they were oriented on the same side of ring A and B. Moreover, H-8 showed NOE correlations with H-11, H-7, and H-14, suggesting that these protons were on the same face of ring B and C. The absence of cross-peaks between δ_H 1.91 (H-10) and δ_H 1.59 (H-11) indicated that these two groups of H-10/H-5/H-2 and H-11/H-8/H-14/H-7 were oriented on the opposite side. A single-crystal X-ray crystallographic analysis of **1** clarified the absolute configuration. The X-ray structure was elucidated using the differences in anomalous dispersion from Cu K_α radiation and allowed unambiguous assignment of the absolute configurations at the 12 chiral centers as 2*S*, 3*S*, 4*R*, 5*R*, 6*R*, 7*R*, 8*S,* 9*R*, 10*S*, 11*R*, 13*R*, and 14*R* (Figure 2). To confirm this assignment, a CD exciton chirality method was applied.[17] The ECD spectrum of **1** (Figure 3) exhibited a positive split between the two

chromophores of the benzoate moiety at C-14 (223 nm, $\Delta\varepsilon$ +3.97, π-π* transition) and the $\Delta^{15,16}$ double bond [6,7,18] (206 nm, $\Delta\varepsilon$ -1.33, π-π* transition), indicating that the transition dipole moments of the two chromophores were oriented in a clockwise manner. Thus, the absolute configuration of the twelve chiral centers in **1** was deduced to be as shown, and this was consistent with the result of the single-crystal X-ray crystallographic analysis (Figure 3). These data corroborated the biogenic method of configurational assignment for the abnormal *R* configuration of the C-7 of neogenkwanine A.

The molecular formula of compound **2**, neogenkwanine B was determined to be $C_{27}H_{36}O_9$ on the basis of the molecular ion peak at *m/z* 527.2251 (calcd 527.2252) in the HRESIMS analysis, indicating 10 degrees of double-bond equivalence. Similar NMR studies were also conducted with **2**, and the ^{1}H NMR and ^{13}C spectra of **2** (Table 1) showed the same characteristics as **1**, and the only difference between them was the linkage site of the benzoyloxy group. In the ^{1}H NMR spectrum of **2**, the H_2-20 at δ_H 4.82 (1H, d, J = 12.0 Hz) and 4.41 (1H, d, J = 12.0 Hz) was downfield shifted ca. $\Delta\delta$ 0.87-0.94 compared with that of **1** (Table 1), indicating that the benzoyloxy group was at C-20 in **2**. In addition, the benzoyloxy site was established unambiguously by a HMBC experiment in which long-range correlations between H_2-20 (δ_H 4.41, 4.82) and C-1′ (δ_C 167.2) were observed. Taking all these spectral features into account, the structure of **2** was unequivocally that shown in Chart **1**. Detailed analysis of the NOESY and the ^{1}H NMR coupling constants of **2** revealed that its relative configuration was consistent with that of **1**.

In order to determine the absolute configuration of **2**, the CD exciton chirality method was applied.[17] The CD spectrum of **2** (Figure 3) showed a negative Cotton effect, which centered around the UV maximum at 227 nm, corresponding to the exciton coupling between the

chromophores of the benzoate moiety at C-20 (232 nm, $\Delta\varepsilon$ −4.68) and the $\Delta^{15,16}$ double bond (207 nm, $\Delta\varepsilon$ +1.87). The counter-clockwise spatial geometry of the two chromophores, thus showed that the absolute configuration of **2** was 2*S*, 3*S*, 4*R*, 5*R*, 6*R*, 7*R*, 8*S,* 9*R*, 10*S*, 11*R*, 13*R*, and 14*R* (Figure 3). This was confirmed by alkaline hydrolysis of **1** and **2** (Scheme 1), which produced the same skeleton, as identified by HRESIMS, NMR, optical rotation and analytical HPLC data. (Experimental Section).

Neogenkwanine C (**3**) had the molecular formula $C_{37}H_{50}O_{10}$, as determined by HRESIMS *m/z*: 677.3294 $[M+Na]^+$ (calcd 677.3296), indicating 13 degrees of double-bond equivelance and 150 mass units heavier than **1**. The ^1H and ^{13}C NMR data (Table 1) of **3** corresponded closely to those of **1**, except for the presence of one additional $C_{10}H_{14}O$ mass unit in **3**, and this was supported by its molecular formula. In the ^1H NMR spectrum of **3**, the H-3 at δ_H 5.18 (1H, d, J = 9.4 Hz) was downfield shifted ca. $\Delta\delta$ 0.95 compared with **1**, indicating that a C_{10} acyl group was located at the C-3 (δ_C 74.2) of **3**, which was further supported by the long-range correlations between H-3 (δ_H 5.18) and C-1′ (δ_C 166.6) in the HMBC spectrum (Figure 16 in ESI †). The 2″*E*, 4″*Z* configuration of the C_{10} acyl group in **3** was confirmed by the ^1H NMR coupling constants ($J_{2'',3''}$ = 15.0 Hz, $J_{4'',5''}$ = 10.9 Hz) and the correlation in its NOESY plot H-2″/H-4″, (Figure 17 in ESI †). Other correlations in the NOESY spectrum were the same as **1** showing that its relative configuration was consistent with that of **1**. The absolute structure of **3** was further identified by a combined analysis involving a CD exciton chirality study and alkaline hydrolysis. The nature of the ECD split of compound **3** (Figure 3), which centered at the UV maximum (ca. λ_{max} = 265 nm), corresponded to the exciton coupling between the two chromophores of 2"*E*, 4"*Z* dienoyl at C-3 (261 nm, $\Delta\varepsilon$ +6.75) and the benzoate moiety at C-14 (231 nm, $\Delta\varepsilon$ −1.35).[7,19] Thus, the absolute configuration of **3** was established by the clockwise nature of the two chromophores as

2*S*, 3*S*, 4*R*, 5*R*, 6*R*, 7*R*, 8*S,* 9*R*, 10*S*, 11*R*, 13*R*, and 14*R*. This was further confirmed by alkaline hydrolysis of **1** and **3** (Scheme 1), which produced **9** as the sole skeleton, and this was confirmed by comparison of HRESIMS, NMR, optical rotation and HPLC data (Experimental Section).

Neogenkwanine D (**4**), showed an $[M + Na]^+$ ion peak at *m/z* 677.3291 in its HRESIMS, corresponding to the molecular formula $C_{37}H_{50}O_{10}$ (calcd for $C_{37}H_{50}O_{10}$, 677.3296). The 1D and 2D NMR spectra of **4** were generally similar to those of **3** (Tables 1), suggesting that **4** is also a daphnane-type diterpene. Compound **4** differed from **3** in the relative configuration of C-4″ as defined by the NOESY data. The correlation between H-3″/H-5″ implied that the configuration of C-4″ in **4** was *E*. Thus, compound **4** was the C-4″ diastereomer of **3**. The structure of **4** was further confirmed by a combined analysis of the NMR, ECD spectra and an alkaline hydrolysis experiment.

The molecular formula of neogenkwanine E (**5**) was assigned as $C_{37}H_{50}O_{10}$ based on a molecular ion peak at *m/z* 677.3291 $[M+Na]^+$ (calcd 677.3296) in its positive mode HRESIMS. The ^1H and ^{13}C NMR spectroscopic pattern of **5** (Table 2) showed similar characteristics to **4**, and the only difference between them was the linkage site of the benzoyloxy group. In the ^1H NMR spectrum of **5**, the H_2-20 at δ_H 4.62 (1H, d, J = 12.0 Hz) and 4.53 (1H, d, J = 12.0 Hz) was downfield shifted ca. $\Delta\delta$ 0.60-1.09 compared with that of **4**, indicating that the benzoyloxy group was located at C-20 in **5** (Table 2). In addition, the benzoyloxy site was established unambiguously by a HMBC experiment in which long-range correlations between H_2-20 (δ_H 4.53, 4.62) and C-1′ (δ_C 167.4) were observed. Taking all these spectral features into account, the structure of **5** was assigned unequivocally as that shown in Chart 1. Detailed analysis of the NMR, ECD spectra and alkaline hydrolysis of **5** revealed that its absolute configuration was consistent with that of **1 (**S46 and S48 in ESI †**)**.

Neogenkwanine F (**6**), showed an $[M + Na]^+$ ion peak at *m/z* 677.3293 in its HRESIMS, corresponding to the molecular formula $C_{37}H_{50}O_{10}$ (calcd 677.3296), indicating 13 degrees of double-bond equivalence. The NMR data of compounds **5** and **6** were similar (Table 2), except for the 2″*E*, 4″*Z* configuration of the C_{10} acyl group ($J_{2'',3''}$ = 15.0 Hz, $J_{4'',5''}$ = 11.4 Hz) in **6**. Therefore, compound **6** was deduced to be the C-4″ diastereomer of **5**, which was confirmed by 2D NMR experiments (Figure 30 in ESI †). The structure of **6** was further identified by a combined analysis of NMR, ECD spectra and alkaline hydrolysis.

The molecular formula of neogenkwanine G (**7**) was determined to be $C_{34}H_{40}O_{10}$, based on HRESIMS results (experimental *m/z* $[M+Na]^+$ at *m/z* 631.2514 (calcd 631.2514). The ^1H and ^{13}C NMR data (Table 2) of **7** corresponded closely to that of **1**, except for the presence of one additional benzoyloxy group in **7**, and this was supported by its molecular formula. In addition, the benzoyloxy site was established unambiguously by the HMBC experiment in which long-range correlations between H_2-20 (δ_H 4.60, 4.30) and C-1″ (δ_C 167.8) were observed. Taking all these spectral features into account, the structure of **7** was unequivocally that shown in Chart 1 (Absolute configuration was reported in Figure 46 and 48 in ESI †), which was further confirmed by analysis of NMR, ECD spectral data and alkaline hydrolysis.

Neogenkwanine H (**8**), was isolated as an amorphous powder and had the same molecular formula of $C_{27}H_{36}O_9$ as that of **1** according to the ^{13}C NMR data and the accurate molecular ion peak of *m/z* $[M+Na]^+$ at *m/z* 527.2255 (calcd 527.2252) in the HRESIMS. The ^1H and ^{13}C NMR data, along with the HSQC spectrum, (Table 2), showed one tertiary methyl at δ_H 1.82 (3H, s), two secondary methyls at δ_H 0.95 (3H, d, J = 6.6 Hz) and 0.91 (3H, d, J = 7.2 Hz), and one oxygenated methylene at δ_H 3.70 (1H, d, J = 12.6 Hz) and 4.00 (1H, d, J = 12.6 Hz). The olefinic H-atoms appeared to be at a terminal double bond [δ_H 5.08 (1H, s) and 5.11 (1H, s); δ_C 114.9 and

144.3], while five aromatic H- C-atoms at δ_H 8.03-7.44 (5H) and δ_C 128.4-133.2 (6C) indicated the presence of one phenyl moiety. The aforementioned data suggested that **8** was also a daphnane-type diterpene with structural features similar to those of **1**, except for the difference in the B-ring and the benzoyloxy site. The HMBC correlation (Figure 4) from H-7 to the carbonyl carbon C-1′ (δ_C166.1) indicated attachment of the benzoyloxy group to C-7. With this pre-condition, the 4,7-ether group in B ring is clearly impossible. Meanwhile, in the ^{13}C NMR spectrum of **8**, the C-6 at δ_C 86.1 was downfield shifted ca. $\Delta\delta$ 2.3 ppm compared with that of **1** (Table 1 and 2), demonstrated that there was a 4,6-ether group in B ring of **8**.

The relative configuration of **8** was elucidated using the NOESY spectrum (Figure 4) and the ^{1}H NMR coupling constants. The correlations of H-2/H-10 and H-10/H-5 revealed the *α*-orientation of these protons. The correlations of H-7/H-8, H-8/H-11 and H-8/H-14 supported the *β*-orientation of these protons. In addition, the absence of cross-peaks between δ_H 1.99 (H-10) and δ_H 1.52 (H-11) indicated that these two groups of H-10/H-5/H-2 and H-11/H-8/H-14/H-7 were located on opposite sides. Furthermore, in the ^{1}H NMR spectrum of **8**, the vicinal coupling constant $J_{(2,3)}$ of 10.2 Hz suggested a *cis* relationship between the protons H-2 and H-3.

In order to determine the absolute configuration of **8**, the CD exciton chirality method was applied.[17] The ECD split manner of compound **8** showed a negative Cotton effect, which centered around the UV maximum at 230 nm, corresponding to exciton coupling between the chromophores of the benzoate moiety at C-7 (225 nm, $\Delta\varepsilon$ −2.14) and the $\Delta^{15,16}$ double bond (209 nm, $\Delta\varepsilon$ +0.52). The counter-clockwise spatial configuration of the two chromophores thus showed that the absolute configuration of **8** was 2*S*, 3*S*, 4*R*, 5*R*, **6*S***, **7*S***, 8*S,* 9*R*, 10*S*, 11*R*, 13*R*, and 14*R* **(**Figure 46 and 48 in ESI †**)**.

It is interesting to note that there appears to be considerable biosynthetic flexibility in the

Thymelaeaceae and Euphorbiaceae families of metabolites. Considering known members of the typical daphnane orthoester with 6,7-epoxy moieties,[1,16] trigochinins A-F,[6,7] and neogenkwanines A–H (**1–8**) were isolated from the above-mentioned families, surmised that a close biogenetic link most likely existed between these three skeletal types [6,7-epoxy, 4,6-ether and 4,7-ether groups (scheme 2)]. Resinferonol (**a**) was proposed as the most probable biosynthetic intermediate. The parent polyolresinferonol is derived by basic hydrolysis of proresiniferatoxin (**b**), a natural daphnane lacking the ring C orthoester group previously isolated from the dried latex of *E. resinifera* Berg. in a plausible biogenetic way.[1,20,21] Oxidative cleavage of a C-6–C-7 bond in resinferonol seems to occur to generate a compound with a 6,7-epoxy moiety, which is obvious in the typical daphnane orthoester series as daphnetoxin (**c**),[22] and is also followed by hydration to give 6*α*,7*β*-dihydroxyl or 6*β*,7*α*-dihydroxyl compounds, such as genkwanine I (**d**) and L (**e**) from *D.genkwa*.[11] However, in the case of a mixture of *α*-and *β*-epoxides (**f**, **g**), only the *α*-epoxide was preferentially attacked by the C4 tertiary alcohol to form compounds with the 4,7-ether or 4,6-ether group.[20,21]

The daphnane diterpene orthoesters (DDOs) have been demonstrated to be powerful anticancer agents,[2] and more recently, DDOs were shown to be a new type of DNA topoisomerase I inhibitor with higher activity than hydroxyl camptothecin (one of the most powerful DNA topo I inhibitors).[10] Meanwhile, our current study indicates that the anti-cancer activity of YHL–14 is mediated by activated p38, which results in Sp1 protein accumulation and transactivation, subsequently leading to p21 gene transcription and protein expression, along with cancer cell G2/M phase growth arrest.[13] As a continuation of these studies, the inhibitory effects of constituents of the flower buds of *D. genkwa* on three different cancer cell lines were examined (Table 3). Compounds **3–5** potently inhibited hepatoma (Hep3B) cell growth, with an

IC_{50} values of 7.61 – 8.35 μM. Indeed, **3–6** (IC_{50} = 27.11 − 58.60 μM) were more effective in inhibiting glioma (U87: a cancer cellline insensitive to chemotherapeutic drugs) than the control, temozolomide (IC_{50} = 217.2 μM). Compounds **1**–**2** and **7–8** were only weakly cytotoxic to HL-60, Hep3B and U87 cell lines. Interestingly compounds **1–7** have structures very similar to the rare 4,7-ether group, except for the different substituent groups at C-3, 14 and 20. Since compounds **3–6**, with a C-3 acyloxy group, exhibited stronger inhibitory effects than compounds **1**, **2** and **7**, without the C-3 substituents, it seems that the inhibition of cancer cells is obviously related to the acyloxy group of C-3. These findings indicate that the linkage site and kinds of the substituent groups are important for the cytotoxic effects of the diterpenes examined in the present study. Further structure activity relationship studies and a thorough investigation of the inhibitory mechanism are warranted.

Experimental

General Experimental Procedures

Optical rotations were measured using a Perkin-Elmer-214-MC polarimeter. The ECD spectra were obtained with a BioLogic MOS-450 spectropolarimeter. 1D and 2D spectra were recorded on a Bruker-ARX-600 spectrometer (600 and 150 MHz) in $CDCl_3$: δ in ppm, J in Hz. High resolution electrospray ionization mass measurements (HRESIMS) were recorded in positive ion mode on a Micro TOF-Q (quadrupole-Time of Flight) instrument with a Bruker ESI source. Semi-Preparative HPLC was carried out using a Hitachi instrument (Japan Analytical Industry Co., Ltd.) fitted with a YMC ODS-A column (5 mm; 250×10mm; YMC, Japan). Column chromatography (CC) was carried out using silica gel (SiO_2; 200-300 mesh; Qingdao Marine Chemical Factory, Qingdao, P. R. China) and reversed phase C_{18} silica gel (60-80 mm; Merck, Germany).

Plant material

The flower buds (6.0 kg) of *Daphne genkwa* were collected in August 2006 from the Sichuan Mianyang area, China, and authenticated by Prof. Qi-Shi Sun, School of Traditional Chinese Materia Medica, Shenyang Pharmaceutical University. A voucher specimen (No. 060812) was deposited at the School of Traditional Chinese Materia Medica, Shenyang Pharmaceutical University.

Extraction and isolation

Air-dried flower buds of *Daphne genkwa* (6.0 kg) were extracted thoroughly with 95% EtOH (50 L×3) at room temperature to obtain a brownish-dark crude extract (638.0 g), which was partitioned between $CHCl_3$ (7.5 L×3) and water (7.5 L). The $CHCl_3$-soluble materials (250.0g) were subjected to silica gel normal phase column chromatography (petroleum ether/AcOEt, 100:1→2:1) to yield 7 fractions, denoted as frs.1–7. Fr.4 (17.0 g) was separated on silica gel column involving elution with a $CHCl_3$/MeOH gradient (100:1→2:1) to give 6 fractions fr.4–1 to fr.4–6. Fr.4–3 (3.1 g) was separated by reversed-phase CC (MeOH/H_2O; 75:25) to yield **3** (25mg), **6** (17mg), **13** (8mg), **14** (13mg) and 1**6** (11mg). The elution fraction fr.4-3 was further subjected to C_{18} HPLC (YMC RP-18 ODS-A, 250×10mm; flow rate 2.0mL/min; UV detection at 220 nm; eluent MeOH/H_2O, 88:12) to yield **4** (16mg), **5** (12 mg), **11** (15 mg), **12** (19 mg) and 1**5** (22 mg). Fr.6 was subjected to silica gel column chromatography ($CHCl_3$/MeOH, 30:1→2:1), and then purified by reversed phase HPLC (MeOH/H_2O, 65:35) to give **1** (80 mg), **2** (45 mg), **7** (15 mg), **8** (8 mg) and **10** (12 mg).

Characteristic data of compounds

Neogenkwanine A (**1**): colorless flaky crystals; $[\alpha]_D^{22}$ −14.9 (*c* 2.2, $CHCl_3$); ECD $\Delta\varepsilon_{206}$ −1.33, $\Delta\varepsilon_{223}$ +3.97, $\Delta\varepsilon_{241}$ −2.15 (1.89×10^{-3} M, MeOH); UV (MeOH) λ_{max} (log ε) 225 (2.49) nm; IR

(KBr) ν_{max} 3452, 1711, 1642, 1600, 1580, 1178 cm^{-1}; ^{1}H and ^{13}C NMR (Table 1); HRESIMS: *m/z* 527.2253 $[M+Na]^+$ (calcd for 527.2252, $C_{27}H_{36}O_9Na$).

Single crystal X-ray diffraction analysis of neogenkwanine A (1). Crystallization of neogenkwanine A (**1**) from n-hexane/ethyl acetate gave flaky cocrystals (1: 1) of **1** and ethyl acetate. All measurements were made on a Bruker SMART APEX-II with a RAPID diffractometer using filtered CuK_α radiation (λ = 1.54187 Å). Crystal data: Formula $C_{27}H_{36}O_9$, Formula weight 504.24, Orthorhombic system, Space group: P 21 21 21, a = 11.7035 (7) Å, b = 12.7664 (9) Å, c = 21.1157 (14) Å, $\alpha = \beta = \gamma = 90.00°$, V = 3154.9 (4) $Å^3$, Z = 4, T = 296 (2) K, d = 1.248 g cm^{-3}, specimen: 0.05×0.20×0.010 mm^3. The total number of independent reflections measured was 9697, 4408 reflections unique, of which 4183 were observed ($|F|^2 \geq 2\sigma|F|^2$). All calculations were performed using Crystal Structure except for refinement, which was performed using a direct method SHELXL-97, expanded by using difference Fourier techniques, and refined by full-matrix least-squares calculations. The non-hydrogen atoms were refined anisotropically, and hydrogen atoms were included at their calculated positions. The final indices were R_1 = 0.0429, wR_2 = 0.1181 ($w = 1/\sigma|F|^2$), S = 1.030. Crystallographic data for neogenkwanine A (**1**) have been deposited at the Shanghai Institute of Pharmaceutical Industry.

Neogenkwanine B (**2**): colorless needle crystals; $[\alpha]_D^{22}$ −39.3 (*c* 1.9, $CHCl_3$); ECD $\Delta\varepsilon_{207}$ +1.87, $\Delta\varepsilon_{232}$ −4.68 (2.0×10^{-3} M, MeOH); UV (MeOH) λ_{max} (log ε) 228 (2.59) nm; IR (KBr) ν_{max} 3438, 1700, 1635, 1579 cm^{-1}; ^{1}H and ^{13}C NMR (Table 1); HRESIMS: *m/z* 527.2251 $[M+Na]^+$ (calcd for 527.2252, $C_{27}H_{36}O_9Na$).

Neogenkwanine C (**3**): white amorphous powder; $[\alpha]_D^{22}$ −18.9 (*c*2.6, $CHCl_3$); ECD $\Delta\varepsilon_{231}$ −1.35, $\Delta\varepsilon_{261}$+6.75 (3.47×10^{-3} M, MeOH); UV (MeOH) λ_{max} (log ε) 228 (2.83), 265 (2.97) nm; IR

(KBr) ν_{max} 3450, 1712, 1645, 1607, 1180 cm^{-1}; ^{1}H and ^{13}C NMR (Table 1); HRESIMS: *m/z* 677.3294 $[M+Na]^+$ (calcd for 677.3296, $C_{37}H_{50}O_{10}Na$).

Neogenkwanine D (**4**): white amorphous powder; $[\alpha]_D^{22}$ −30.6 (*c* 1.2, $CHCl_3$); ECD $\Delta\varepsilon_{223}$ −0.96, $\Delta\varepsilon_{263}$ +5.38 (2.17×10^{-3} M, MeOH); UV (MeOH) λ_{max} (log ε) 226 (2.81), 262 (2.88) nm; IR (KBr) ν_{max}3431, 1705, 1635, 1592, 1166 cm^{-1}; ^{1}H and ^{13}C NMR (Table 1); HRESIMS: *m/z* 677.3291 $[M+Na]^+$ (calcd for 677.3296, $C_{37}H_{50}O_{10}Na$).

Neogenkwanine E (**5**): white amorphous powder; $[\alpha]_D^{22}$ −22.5 (*c* 1.3, $CHCl_3$); ECD $\Delta\varepsilon_{251}$ −3.80 (1.36×10^{-3} M, MeOH); UV (MeOH) λ_{max} (log ε) 214 (2.73), 258 (2.75) nm; IR (KBr) ν_{max} 3451, 1718, 1641, 1603, 1168 cm^{-1}; ^{1}H and ^{13}C NMR (Table 2); HRESIMS: *m/z* 677.3291 $[M+Na]^+$ (calcd for 677.3296, $C_{37}H_{50}O_{10}Na$).

Neogenkwanine F (**6**): white amorphous powder; $[\alpha]_D^{22}$ −19.3 (*c* 1.8, $CHCl_3$); ECD $\Delta\varepsilon_{245}$ −3.38 (1.05×10^{-3} M, MeOH); UV (MeOH) λ_{max} (log ε) 219 (2.63), 263 (2.67) nm; IR (KBr) ν_{max} 3447, 1711, 1643, 1600, 1176 cm^{-1}; ^{1}H and ^{13}C NMR (Table 2); HRESIMS: *m/z* 677.3293 $[M+Na]^+$ (calcd for 677.3296, $C_{37}H_{50}O_{10}Na$).

Neogenkwanine G (**7**): white amorphous powder; $[\alpha]_D^{22}$ −35.1 (*c* 1.0, $CHCl_3$); ECD $\Delta\varepsilon_{235}$ +5.15 (4.50×10^{-3} M, MeOH); UV (MeOH) λ_{max} (log ε) 233 (2.57) nm; IR (KBr) ν_{max} 3452, 1720, 1645cm^{-1}; ^{1}H and ^{13}C NMR (Table 2); HRESIMS: *m/z* 631.2514 $[M+Na]^+$ (calcd for 631.2514, $C_{34}H_{40}O_{10}Na$).

NeogenkwanineH (**8**): white amorphous powder; $[\alpha]_D^{22}$ −24.7 (*c* 1.5, $CHCl_3$); ECD $\Delta\varepsilon_{225}$ −2.14, $\Delta\varepsilon_{243}$ +1.52 (1.90×10^{-3} M, MeOH); UV (MeOH) λ_{max} (log ε) 230 (2.82) nm; IR (KBr) ν_{max} 3441, 1708, 1645, 1602, 1178 cm^{-1}; ^{1}H and ^{13}C NMR (Table 2); HRESIMS: *m/z* 527.2255 $[M+Na]^+$ (calcd for 527.2252, $C_{27}H_{36}O_9Na$)

Alkaline Hydrolysis of Compounds 1−7

Compound **1** (15 mg) was dissolved in MeOH-H_2O (10.0 mL), and 0.01 M NaOH (0.8 mL) was added. The reaction mixture was stirred at room temperature for 4.0 h until all the starting material had disappeared, as observed by TLC. Neutralization was carried out using dilute HCl, and the residue was dried under vacuum and then extracted with CH_2Cl_2 (3 × 8 mL).[23] The organic layer was concentrated under reduced pressure and the residue was purified by HPLC on a Dikma Diamonsil C_{18} column (4.6 mm×150 mm, 5 μm) with isocratic elution using MeOH−H_2O (1:1) and a flow rate of 1.0 mL/min (sample injection, 20 μL; concentration, 0.03 mg/μL) to afford pure compound **9** (6.2 mg). Derivatives **2**−**7** were also hydrolyzed, and the reaction residues were purified using the same procedures as described above to yield compound **9**.

Compound **9**. white amorphous powder; $[\alpha]_D^{22}$ −25.3 (*c* 0.7, $CHCl_3$); HRESIMS: *m/z* 423.1975 $[M+Na]^+$ (calcd for 423.1989, $C_{20}H_{32}O_8Na$). ^{1}H NMR (600 MHz, $CDCl_3$): δ 1.88 (1H, m, Ha-1), 1.18 (1H, m, Hb-1), 2.30 (1H, m, H-2), 4.23 (1H, d, *J* = 10.2 Hz, H-3), 4.94 (1H, s, H-5), 4.09 (1H, s, H-7), 2.23 (1H, brs, H-8), 1.83 (1H, m, H-10), 1.51 (1H, brs, H-11), 1.80 (1H, m, Ha-12), 1.75 (1H, m, Hb-12), 4.11 (1H, brs, H-14), 5.12, 5.11 (each 1H, s, H_2-16), 1.84 (3H, s, CH_3-17), 0.84 (3H, d, *J* = 7.2 Hz, CH_3-18), 0.95 (3H, d, *J* =5.7 Hz, CH_3-19), 4.31 (1H, d, *J* = 12.0 Hz, Ha-12), 4.12 (1H, d, *J* = 12.0 Hz, Hb-12); ^{13}C-NMR (150 MHz, $CDCl_3$): δ34.2 (C-1), 32.1 (C-2), 75.0 (C-3), 91.2 (C-4), 83.5 (C-5), 83.4 (C-6), 80.7 (C-7), 44.8 (C-8), 73.4 (C-9), 47.7 (C-10), 36.0 (C-11), 36.5 (C-12), 74.3 (C-13), 72.0 (C-14), 144.9 (C-15), 115.0 (C-16), 19.4 (C-17), 13.9 (C-18), 16.1 (C-19), 65.8 (C-20).

Material and methods for growing cells and cell screening

The cancer cell growth inhibitory activity of compounds **1**–**8** was measured by the MTT method. Three human cancer cell lines (ATCC) were used: hepatoma: Hep3B, glioma: U87, and

leukemia: HL-60 (Table 3). Tested compounds were dissolved in DMSO and the final concentration of DMSO in the culture medium was kept below 0.1% (*v/v*). Cultivated HL-60, Hep3B or U87 cells were seeded in 96-well plates with 1×10^4 cells/well. Cells were incubated in a humidified atmosphere with 5% CO_2 at 37 ^oC for 24 h to allow them to recover and reattach before drug addition. Triplicate samples of each tumor cell line were exposed to the tested compounds at different concentrations for 48 h, with 5-fluorouracil and temozolomide (Shanghai Sunrise Enterprises Co., Ltd.) as positive controls. After incubation, MTT solution (0.25 mg/mL in PBS) was added (10 μL/well) and the plates were incubated for an additional 4h at 37 ^oC. The produced formazan crystals were dissolved in 100 μL DMSO and the optical density of the solution was measured at 492 nm using a microplate reader (Synergy HT (Biotek)), The IC_{50} values of compounds **1–8** were then calculated using SPSS (18.0) software.

Conclusions

In summary, eight daphnane-type diterpenes neogenkwanines A–H (**1–8**), together with seven known ones (**10–16**), were isolated from *Daphne genkwa*. The new structures were determined by extensive spectroscopic analyses, and their absolute congurations were assigned by single-crystal X-ray diffraction, CD exciton chirality data and hydrolysis experiments. Note that, this is the first report that the daphnane-type diterpenes featuring an unusual 4,7-ether group and the close biosynthetic relationships among these three skeletal daphnane-types (6,7-epoxy, 4,6-ether and 4,7-ether groups). Furthermore, cytotoxicity of all these compounds was evaluated on three cells. Among them, compounds **3, 4** and **5** exhibited significant inhibitory effects against Hep3B cell lines, **3–6** were more effective in inhibiting U87 than temozolomide (the control). The inhibitory mechanism of the active metabolites is under investigation in our laboratory and will be reported in due course.

Acknowledgement

Financial support from the National Nature Science Foundation (30973868, 81273388) of P. R. China and the Foundation (F11-265-6-01) from the Project of Science and Technology of Shenyang of P. R. China are gratefully acknowledged. We thank Professor Qi-shi Sun and Doctor Jia-Liang Zhong for identification of the plant material and single crystal X-ray diffraction analysis respectively.

Notes and references

1 W. D. He, M. Cik, G. Appendino, L. V. Puyvelde, J. E. Leysen, N. De Kimpe, *Mini-Rev. Med. Chem.*, 2002, **2**, 185–200.

2 S. G. Liao, H. D. Chen, J. M. Yue, Chem. Rev., 2009, **109**, 1092–1140.

3 W. D. He, M. Cik, L. V. Puyvelde, J. V. Dun, G. Appendino, A. Lesage, I. V. der Lindin, J. E. Leysen, W. Wouters, S. G. Mathenge, F. P. Mudida, N. De Kimpe, *Bioorg. Med. Chem*., 2002,**10**, 3245–3255.

4 E. Stanoeva, W. D. He, N. De Kimpe, *Bioorg. Med. Chem*., 2005, **13**,17–28.

5 W. D. He, M. Cik, A. Lesage, I. V. der Lindin, N. De Kimpe, G. Appendino, J. Bracke, S. G. Mathenge, F.P. Mudida, J. E. Leysen, L. V. Puyvelde, *J .Nat. Prod*., 2000, **63**, 1185-1187.

6 H. D. Chen, X. F. He, J. Ai, M. Y. Geng, J. M. Yue, *Org. Lett.,* 2010, **12**, 1168–1171.

7 H. D. Chen, S. P. Yang, X. F. He, H. B. Liu, J. Ding, J. M. Yue, *Tetrahedron,* 2010, **71**, 1573–1578.

8 W. C. Wang, S. R. Shen, *Reprod. Contracept.,* 1988, **8**, 60–61.

9 C. R. Wang, B. N. Zhou, Z. P. Gu, *Reprod. Contracept.,* 1989, **9**, 9−11.

10 S. X. Zhang, X. N. Li, F. H. Zhang, P. W. Yang, X. J. Gao, Q. L. Song, *Bioorg. Med. Chem.,* 2006, **14**, 3888–3895.

11 Z. J. Zhan, Q. F. Chen, J. M. Yue, *Bioorg. Med. Chem.,* 2005, **13**, 645–665.

12 L. Z. Li, P. Y. Gao, Y. Peng, L. H. Wang, J. Y. Yang, C. F. Wu, Y. Zhang, S. J. Song, *Helv. Chim. Acta.,* 2010, **93**, 1172–1179.

13 R. W. Zhang, Y. L. Wang, J. X. Li, H. L. Jin, S. J. Song, C. S. Huang, *J. Biolog. Chem.,* 2014, **289**, 6394–6403.

14 C. R. Wang, Z. X. Chen, B. P. Ying, B. N. Zhou, J. S. Liu, B. C. Pan, *Acta Chim. Sin.,* 1981, **39**, 422–425.

15 O. HaJime, H. Misuru, O. Takanao, K. Koichi, F. Hirota, S. Masami, Y. Ziro, S. Takashi, *Agric. biol. chem.*, 1982, **46**, 3605–2608.

16 G. H. Stout, W. G. Balkenhol, M. Poling, G. L. Hickernell, *J. Am. Chem. Soc.,* 1970, **92**, 1070–1071.

17 N. Berova, K. Nakanishi, R. W. Woody, in *Circular Dichroism: Principles and Applications.* Wiley-VCH, New York, 2000, pp. 337–382.

18 N. Harada, J. Iwabuchi, Y. Yokota, H. Uda, K. Nakanishi, *J. Am. Chem. Soc.,* 1981, **103**, 5590−5591.

19 X. D. Guo, F. Xiang, X. N. Wang, H. Q. Yuan, G. M. Xi, Y. Y. Wang, W. T. Yu, H. X. Lou, *Phytochemistry,* 2010, **71**, 1573–1578.

20 M. Hergenhahn, W. Adolf, E. Hecker, *Tetrahedron Lett.,* 1975, (**19**/**20**), 1595−1598.

21 R. J. Schmidt, F. J. Evans, *Phytochemistry,* 1976, **15**, 1778−1779.

22 T. C. Michael, S. S. Christina, C. M. Mark, *Org. Lett.,* 2011, **13**, 4890–4893.

23 X. Y. Chen, H. Q. Wang, T. Zhang, C. Liu, J. Kang, R. Y. Chen, D. Q. Yu, *J. Nat. Prod.,* 2013, **76**, 1528−1534.

Figure captions

Chart 1 Structure of compounds **1**–**16**.

Figure 1. Selected HMBC correlations of **1**. (left). Selected NOESY correlations and relative configuration of **1** (right).

Figure 2. ORTEP drawing of neogenkwanine A (**1**).

Figure 3. Experimental ECD (in MeOH) of **1**–**3**. Bold lines denote the electric transition dipole of the chromophores for **1**–**3**. Stereoviews of compounds **1**–**3.**

Figure 4. Selected HMBC correlations of **8** (left). Selected NOESY correlations and relative configuration of **8** (right).

Scheme 1. Hydrolysis of **1**−**7**

Scheme 2. Relationship between the Proposed Biogentic Link to Compounds Furnished with 6,7-epoxy, 4,6-ether and 4,7-ether groups.

Table 1.[1]H (600 MHz) and [13]C (150 MHz) NMR ($CDCl_3$) Data for neogenkwanines A–D (**1–4**)

No	neogenkwanine A		neogenkwanine B		neogenkwanine C		neogenkwanine D	
	δ_H, mult (*J* in Hz)	δ_C	δ_H, mult (*J* in Hz)	δ_C	δ_H, mult (*J* in Hz)	δ_C	δ_H, mult (*J* in Hz)	δ_C
1a 1b	1.85, m 1.18, m	34.9	1.88, m 1.18, m	34.1	1.32, m 1.26, m	33.9	1.32, m 1.27, m	33.9
2	1.97, m	31.9	2.29, m	31.9	2.31, m	34.4	1.87, m	34.7
3	4.23, d, (10.2)	74.3	4.23, d, (10.2)	74.1	5.18, d, (10.2)	74.7	5.14 , d, (10.2)	74.7
4		90.4		90.8		91.3		91.5
5	4.59, s	85.1	5.02, s	83.1	4.58, s	84.8	4.58 , s	84.8
6		83.8		83.0		82.3		83.8
7	3.90, s	80.5	4.16, d, (3.0)	81.0	3.88, d, (2.6)	80.3	3.90, s	80.6
8	2.46, brs	45.8	2.15, brs	44.5	2.44, brs	46.1	2.43, brs	46.3
9		71.8		73.1		71.4		71.8
10	1.93, m	49.0	1.84,m	47.7	2.03, m	52.5	2.10, m	52.3
11	1.58, m	35.8	1.50, m	36.4	1.60, m	36.7	1.38, m	36.8
12a 12b	2.33, m 2.13, m	35.9	1.85, m 1.77, m	35.7	2.31, m 2.15, m	36.2	2.13, m 2.10, m	36.4
13		74.2		74.8		74.2		74.5
14	5.79, brs	72.2	4.10, brs	72.0	5.79, brs	72.2	5.77, brs	72.4
15		144.8		144.7		144.8		145.1
16	5.20, s; 5.19, s	114.9	5.12, s; 5.11, s	114.8	5.18, s; 5.19, s	114.9	5.15, s; 5.17, s	115.1
17	1.92, s	19.2	1.82, s	19.1	1.91, s	19.2	1.8, s	19.3
18	0.96, d, (6.6)	13.6	0.84, d, (7.2)	13.8	1.0, d, (6.0)	14.0	0.95, d, (6.3)	14.0
19	0.98, d,(7.2)	15.9	0.95, d, (6.6)	16.0	1.0, d, (6.0)	15.0	0.93, d, (6.6)	15.4
20a 20b	3.95, d,(11.4) 3.47, d,(11.4)	67.1	4.82, d,(12.0) 4.41, d, (12.0)	67.4	3.93, d, (11.3) 3.44, d, (11.3)	67.4	3.82, d, (12.0) 3.44, d, (12.0)	67.5
1′		166.6		167.2		166.6		168.3
2′		130.0		129.9		130.4		130.7
3′, 7′	8.03, m	129.6 129.6	8.01, m	129.6 129.6	8.02, m	129.6 129.6	8.02, m	129.8 129.8
4′, 6′	7.45, m	128.6 128.6	7.42, m	128.5 128.5	7.45, m	128.6 128.6	7.31, m	128.8 128.8
5′	7.56, m	133.0	7.55, m	133.3	7.56, m	133.0	7.53, m	133.2
1″						167.0		166.9
2″					5.93, d, (15.0)	119.8	5.80, d, (15.0)	118.6
3″,					7.67,dd, (11.5,15.0)	143.1	7.26, m	147.1
4″					6.13, dd, (10.9, 11.5)	126.2	6.17, m	128.4
5″					5.92, m	141.3	6.14, m	146.5
6″					1.90, m	28.3	2.17, m	33.3
7″					1.43, m	28.9	1.42, m	28.6
8″					1.34, m	31.4	1.34, m	31.6
9″					1.31, m	22.5	1.29, m	22.7
10″					0.89, t, (6.6)	13.9	0.90, t, (6.6)	14.0

Table 2. ^{1}H (600 MHz) and ^{13}C (150 MHz) NMR ($CDCl_3$) Data for neogenkwanines E–H (**5**−**8**)

No	neogenkwanine E		neogenkwanine F		neogenkwanine G		neogenkwanine H	
	δ_H, mult (J in Hz)	δ_C	δ_H, mult (J in Hz)	δ_C	δ_H, mult (J in Hz)	δ_C	δ_H, mult (J in Hz)	δ_C
1a 1b	2.49, m 2.25, m	33.8	1.99, m 1.96, m	33.8	1.97, m 1.23, m	35.2	1.91, m 1.12, m	35.1
2	1.99, m	31.8	1.87, m	31.8	2.34, m	32.3	2.22, m	31.6
3	5.25 , d, (10.2)	74.3	5.25, d, (10.2)	74.3	4.23, d, (10.2)	74.5	4.22 , d, (10.2)	73.5
4		91.6		91.0		90.5		95.3
5	5.07, s	81.0	5.14, s	81.0	4.74, s	84.5	5.51, s	73.6
6		82.2		82.3		83.5		86.1
7	4.20, s	79.3	4.25, s	79.5	4.30, s	80.6	5.91, s	75.3
8	2.24, brs	44.3	2.24 , brs	44.3	2.56, brs	45.7	2.50, brs	41.2
9		72.9		72.8		72.5		77.0
10	1.95, m	48.5	1.94, m	48.5	1.98, m	49.2	1.99, dd, (13.8, 6.0)	48.2
11	1.34, m	36.5	1.30, m	36.5	1.54, m	35.9	1.52, m	36.1
12a 12b	1.93, m 1.59, m	34.8	1.89, m 1.80, m	34.8	2.10, m 1.78, m	35.6	1.85, m 1.60, m	33.5
13		74.3		74.3		74.8		74.9
14	4.21, brs	72.1	4.21, brs	72.1	5.91, brs	72.6	4.36, brs	75.3
15		145.8		145.9		145.5		144.3
16	5.13, s; 5.16, s	113.1	5.12, s; 5.15, s	113.1	5.18, s; 5.19, s	114.9	5.11, s; 5.08, s	114.9
17	1.87, s	17.9	1.86, s	17.9	1.91, s	19.5	1.82, s	19.1
18	0.92, d, (6.3)	12.9	0.89,d,(6.6)	12.9	0.91, d (6.6)	13.8	0.95, d, (6.6)	15.4
19	0.94 , d, (6.6)	15.3	0.84,d, (7.2)	15.3	0.98, d (7.2)	16.2	0.91, d, (7.2)	15.7
20a 20b	4.62, d, (12.0) 4.53, d, (12.0)	67.3	4.72, d, (12.0) 4.40, d, (12.0)	67.2	4.60,d (12.3) 4.30, d (12.3)	67.6	4.00, d, (12.6) 3.70, d, (12.6)	63.2
1′		166.8		166.7		166.6		166.1
2′		130.3		130.3		130.2		130.2
3′, 7′	8.11, m	129.1 129.1	8.08, m	129.2 129.2	7.92, d (8.4)	129.9 129.9	8.02, m	129.9 129.9
4′, 6′	7.40, m	128.3 128.3	7.50, m	128.2 128.2	7.38, m	128.8 128.8	7.42, m	128.4 128.4
5′	7.63, m	132.9	7.63, m	132.9	7.50, m	133.4	7.55, m	133.2
1″		167.4		167.2		167.8		
2″	5.85, d, (15.3)	118.6	5.87, d, (15.0)	120.7		130.0		
3″,	7.35, dd, (15.3, 11.4)	145.9	7.70, dd, (15.0, 11.7)	139.8	8.05, d (8.5)	130.3		
4″	6.26, m	128.2	6.18, dd, (11.7, 11.4)	126.3	7.50, m	128.6		
5″	6.27, m	145.0	5.87, m	141.5	7.60, m	133.6		
6″	2.21, m	32.6	2.24, m	27.7	7.50, m	128.6		
7″	1.47, m	28.2	1.39, m	28.8	8.05, d (8.5)	130.3		
8″	1.34, m	31.1	1.29, m	31.1				
9″	1.29, m	22.2	1.23, m	22.1				
10″	0.92, t, (6.6)	12.8	0.81, t, (6.6)	12.6				

Table 3. Cytotoxicity of Compounds **1**–**8** (IC_{50} in μM)

Cancer cell lines	Hep3B	U87	HL-60
1	>100	>100	>100
2	>100	>100	>100
3	8.35	27.11	10.59
4	8.16	30.80	10.07
5	7.61	47.60	11.17
6	17.61	58.60	12.26
7	>100	>100	>100
8	>100	>100	>100
5-Fu[a]	7.64	–	12.90
TMZ[b]	–	217.2	–

[a]**5-Fu**: 5-fluorouracil as a positive control.
[b]**TMZ**: temozolomide as a positive control.

Chart 1.

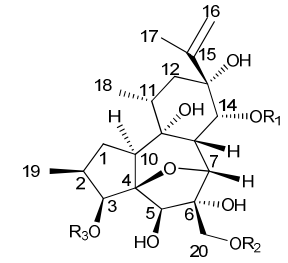

1 R_1=GRP_1 R_2=H R_3=H
2 R_1=H R_2=GRP_1 R_3=H
3 R_1= GRP_1 R_2= H R_3=GRP_3
4 R_1= GRP_1 R_2=H R_3=GRP_2
5 R_1=H R_2=GRP_1 R_3=GRP_2
6 R_1=H R_2= GRP_1 R_3=GRP_3
7 R_1= GRP_1 R_2= GRP_1 R_3=H
9 R_1=H R_2=H R_3=H

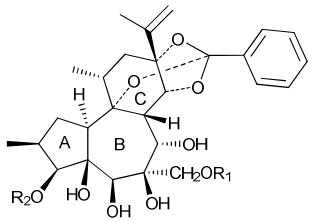

10 R_1=H R_2=H R_3=H
11 R_1= GRP_1 R_2= H R_3=H
12 R_1=H R_2=GRP_1 R_3=H

GRP_1=

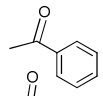

GRP_2=

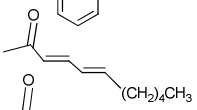

GRP_3=

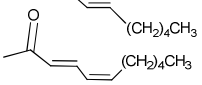

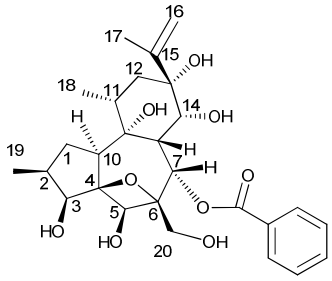

8

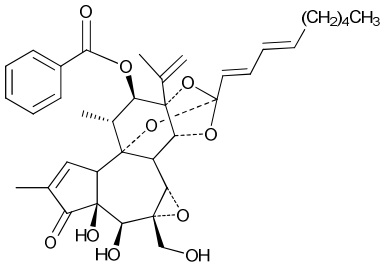

13

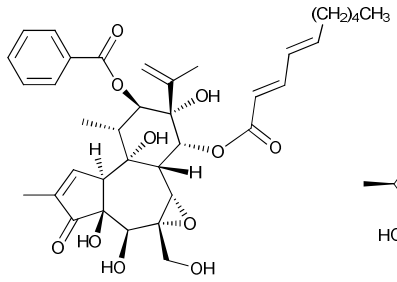

14

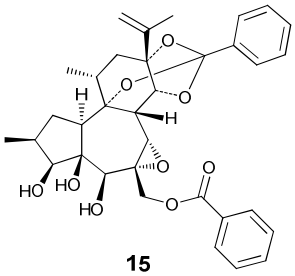

15

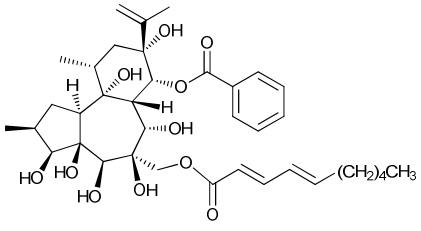

16

Figure 1.

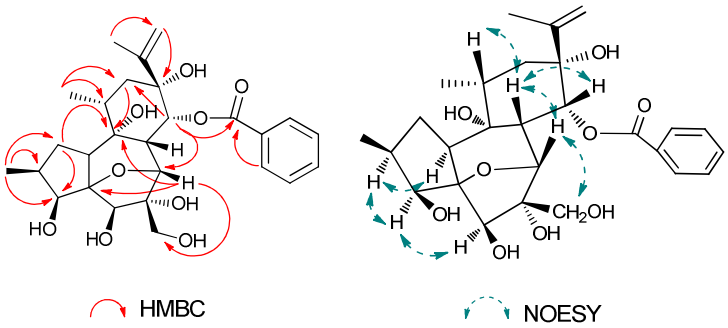

Figure 2.

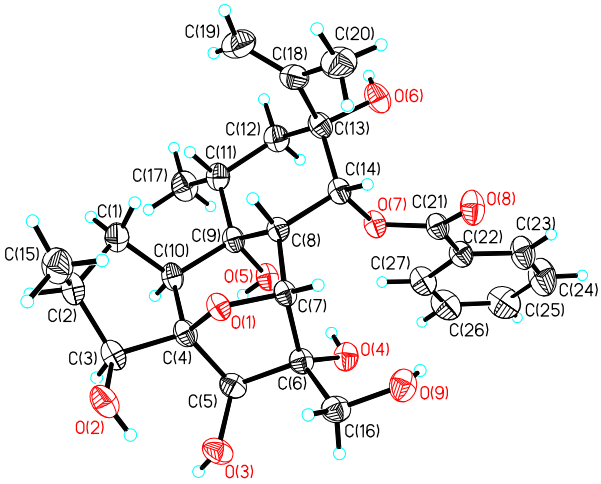

Figure 3.

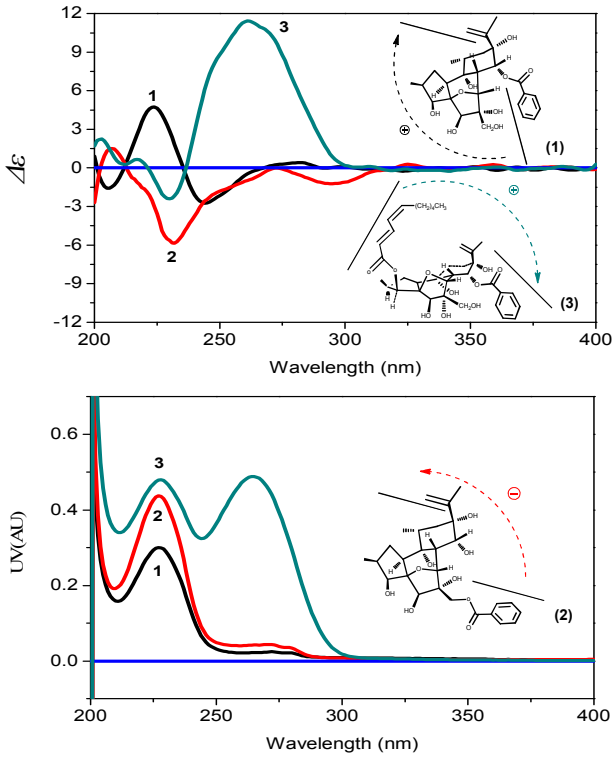

Figure 4.

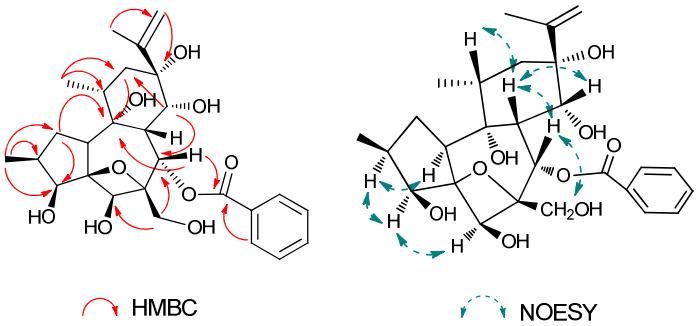

Scheme 1.

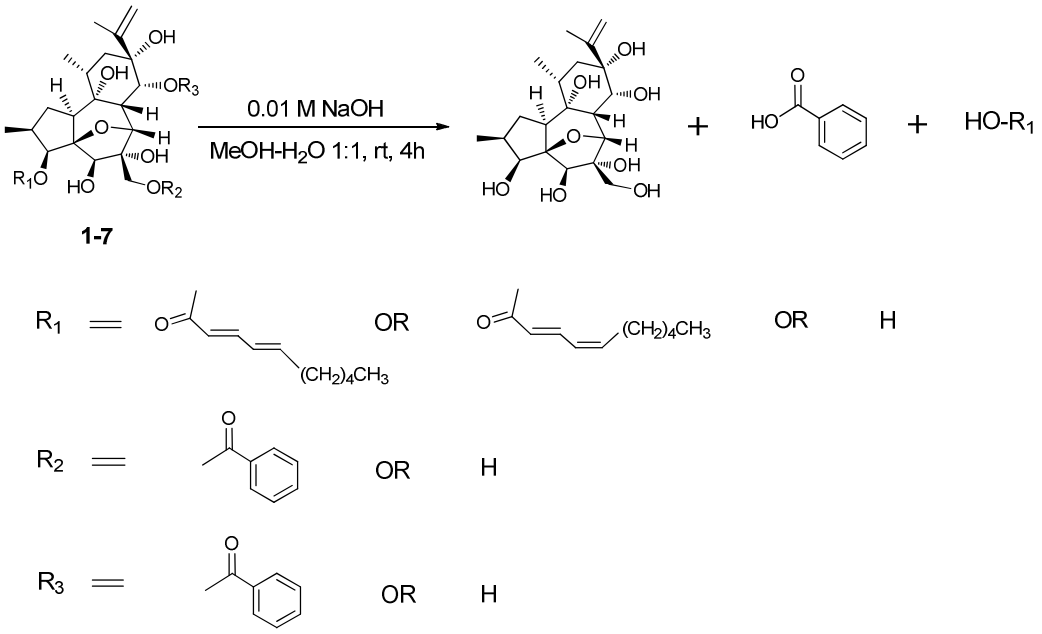

Scheme 2.